Applied Catalysis B: Environmental 144 (2014) 75–82

Contents lists available at ScienceDirect

Applied Catalysis B: Environmental

journal homepage: www.elsevier.com/locate/apcatb

Enhanced photoinduced stability and photocatalytic activity of AgBr photocatalyst by surface modification of Fe(III) cocatalyst

Huogen Yu[a,b,*], Linli Xu[a], Ping Wang[a], Xuefei Wang[a], Jiaguo Yu[c]

[a] Department of Chemistry, School of Science, Wuhan University of Technology, Wuhan 430070, People's Republic of China
[b] State Key Laboratory of Silicate Materials for Architectures, Wuhan University of Technology, Wuhan 430070, People's Republic of China
[c] State Key Laboratory of Advanced Technology for Material Synthesis and Processing, Wuhan University of Technology, Wuhan 430070, People's Republic of China

ARTICLE INFO

Article history:
Received 13 March 2013
Received in revised form 4 June 2013
Accepted 21 June 2013
Available online 29 June 2013

Keywords:
Photocatalysis
Cocatalyst
Fe(III)
Photoinduced stability
Enhancement

ABSTRACT

Recently, AgBr material was demonstrated to be a new and efficient visible-light photocatalyst for the decomposition of various organic compounds. Owing to its excellent photosensitive properties, however, AgBr phase is unavoidably decomposed into metallic Ag under visible-light irradiation, resulting in an obvious destroy of its surface structure. In this study, Fe(III) cocatalyst was grafted on the surface of AgBr particles to form Fe(III)/AgBr photocatalysts by an impregnation method and their photocatalytic performance was evaluated by the photocatalytic decolorization of methyl orange solution under visible-light irradiation. It was found that the Fe(III) cluster could act as a new and effective cocatalyst not only to improve the photocatalytic activity of AgBr photocatalyst, but also remarkably enhance the photoinduced stability of photosensitive AgBr. After surface coating by Fe(III) cocatalyst (8.2 at.%), the photocatalytic activity of AgBr photocatalyst can be greatly improved by a factor of 73% even after five cycles of photocatalytic reactions. Simultaneously, the decomposed amount of AgBr can be significantly deduced from 8.8 at.% to 2.9 at.% by the surface loading of Fe(III) cocatalyst. On the basis of the experimental results, an possible mechanism for the enhanced photocatalytic activity and photoinduced stability of AgBr by Fe(III) cocatalyst was proposed. Compared with the well-known noble metal cocatalysts (e.g., Pt, Au, Ag), the present abundant and cheap Fe(III) cocatalyst can be regarded as one of the ideal cocatalyst for the smart design and development of high-performance photocatalytic materials in various potential applications.

1. Introduction

Developing stable and effective photocatalytic materials for the elimination of organic pollutants has been demonstrated to be one of the important investigation objectives in photocatalysis [1–3]. TiO_2, a traditional photocatalyst, was widely investigated because of its non-toxicity and long-term stability [4–6]. However, the TiO_2 photocatalyst still cannot be widely used in practical applications due to its limited visible-light absorption and low photocatalytic performance. Thus, it is highly required to develop new and highly efficient visible-light-responded photocatalytic materials. Recently, various Ag-based compounds such as AgCl [7–9], AgBr [10–12], AgI [13,14], and Ag_3PO_4 [15,16] were demonstrated to be a new family of highly efficient visible-light photocatalytic materials. In our previous studies, we have also reported the highly efficient Ag-based photocatalytic materials such as Ag_2O [17], Ag_2CO_3 [18], Ag_3PO_4 [19,20], AgCl [21–23], and AgI [24]. Compared with the typical N-TiO_2 visible-light photocatalyst, it is found that the Ag-based photocatalysts usually show a significantly higher photocatalytic performance for the decomposition of various organic substances in aqueous solution [21]. However, it is very interesting and highly required to further improve their photocatalytic performance from the view point of potential applications. In addition, compared with the well-known photocatalytic materials such as TiO_2, one of the obvious disadvantages is that the photoinduced stability of bare Ag-based photocatalysts is quite poor owing to its strong photosensitivity, resulting in an obvious destroy of its surface structure under light irradiation. Unfortunately, less investigation about the enhanced photoinduced stability of photosensitive Ag-based materials has been concerned.

Silver halides (AgX, X = Cl, Br and I), a family of excellent photosensitive Ag-based material, have been extensively used in photographic films for the formation of latent image via their photoinduced decomposition mechanism [25]. Therefore, the

* Corresponding author at: Department of Chemistry, School of Science, Wuhan University of Technology, Wuhan 430070, People's Republic of China.
Tel.: +86 27 87871029; fax: +86 27 87879468.
E-mail address: yuhuogen@whut.edu.cn (H. Yu).

0926-3373/$ – see front matter © 2013 Elsevier B.V. All rights reserved.
http://dx.doi.org/10.1016/j.apcatb.2013.06.023

photosensitive silver halides are unavoidably decomposed into metallic Ag under visible-light irradiation. By absorbing incident light, the photoinduced electrons and holes are generated in the conduction band (CB) and valence band (VB) of silver halides, respectively. The photogenerated electrons in the CB can be captured by surface lattice Ag^+ ions to form metallic Ag_n clusters, whereas the photogenerated holes oxidize lattice X^- to release X_2, resulting in the photodecomposition of silver halides and the formation of metallic Ag. As a consequence, it can be expected that if the photogenerated electrons in the CB of AgX can be quickly captured by other electron accepters before reducing the lattice Ag^+, it is possible for us to improve the photoinduced stability of photosensitive AgX phase. Considering the fact that the photogenerated electrons in the CB of semiconductors can be rapidly transferred via the surface modification of cocatalysts (such as Au, Pt, Ag, and graphene) [26–29], it is quite possible that the photoinduced stability of photosensitive AgX can be greatly enhanced by loading effective cocatalysts on the surface of AgX.

In our previous studies, the Fe(III) cluster was demonstrated to be one of the new and efficient cocatalysts to greatly improve the photocatalytic performance of TiO_2 [30]. Compared with the expensive noble-metal nanoparticles, the Fe element is nontoxic and abundant in natural resources. In this study, Fe(III) cocatalyst was grafted on the surface of AgBr particles to form Fe(III)/AgBr photocatalysts by an impregnation method and their photocatalytic performance was evaluated by the photocatalytic decolorization of methyl orange solution under visible-light irradiation. The effect of Fe(III) cocatalyst on the photocatalytic activity and photoinduced stability of AgBr particles was investigated. It was found that the Fe(III) cluster could act as a new and effective cocatalyst not only to improve the photocatalytic activity of AgBr photocatalyst, but also remarkably enhance the photoinduced stability of photosensitive AgBr. To the best of our knowledge, this is the first report about the enhanced photocatalytic activity and photoinduced stability of AgBr photocatalyst by Fe(III) cocatalyst. Compared with the well-known noble metal cocatalysts (e.g., Pt, Au, Ag), the present abundant and cheap Fe(III) cocatalyst can be regarded as one of the ideal cocatalysts for the smart design and development of high-performance photocatalytic materials. In addition, considering the effective inhibition effect for the rapid decomposition of photosensitive AgBr material by surface cocatalyst, the work may provide a new insight for the potential applications of various photosensitive Ag-based materials.

2. Experimental

2.1. Synthesis of AgBr photocatalyst

The starting aqueous solutions of $AgNO_3$ solution (0.1 mol L^{-1}) and NaBr solution (0.1 mol L^{-1}) were first prepared. The synthesis of AgBr powder was prepared by a simple participation reaction between Ag^+ and Br^- ions in the solution. In a typical synthesis, 35 mL $AgNO_3$ solution was poured into 35 mL of NaBr solution under stirring. After stirring for 5 min, the resultant yellow suspension was maintained at 60 °C for 2 h. The resultant powder was recovered by filtration, rinsed with distilled water, and dried at room temperature.

2.2. Modification of AgBr photocatalyst by Fe(III) cocatalyst

The Fe(III)/AgBr photocatalyst was prepared by an impregnation technique. In a typical preparation, 0.5 g of AgBr powder was dispersed into 75 mL $Fe(NO_3)_3$ solution under stirring. After stirring for 15 min, the suspension solution was maintained at 60 °C for 2 h. The resultant powder was recovered by filtration, rinsed with distilled water, and dried at 60 °C to obtain modified Fe(III)/AgBr photocatalysts. To investigate the effect of $Fe(NO_3)_3$ concentration on the microstructures and photocatalytic performance of AgBr photocatalyst, the $Fe(NO_3)_3$ concentration was controlled to be 0.001, 0.005, 0.01, and 0.05 mol L^{-1}, and the resultant Fe(III)/AgBr photocatalyst can be referred to as Fe(III)/AgBr (0.001 M), Fe(III)/AgBr (0.005 M), Fe(III)/AgBr (0.01 M), and Fe(III)/AgBr (0.05 M), respectively.

For comparison, the bare AgBr were also treated in distilled water under an identical experimental condition.

2.3. Characterization

X-ray diffraction (XRD) patterns were obtained on a D/MAX-RBX-ray diffractometer (Rigaku, Japan). X-ray photoelectron spectroscopy (XPS) measurements were done on a KRATOA XSAM800 XPS system with Mg Kα source. All the binding energies were referenced to the C 1s peak at 284.8 eV for the surface adventitious carbon. Morphological analysis was performed with an S-4800 field emission scanning electron microscope (FESEM) (Hitachi, Japan) with an acceleration voltage of 10 kV. UV–vis absorption spectra were obtained using a UV–visible spectrophotometer (UV-2550, SHI-MADZU, Japan).

2.4. Photocatalytic activity

MO is a simple azo dye that has been widely used as a model system to probe the photocatalytic performance of various photocatalysts [21]. It is generally considered to be very stable to light and difficult to decompose, though MO can absorb visible light at ca. 464 nm. The photocatalytic activity of the prepared samples was performed at ambient temperature. Experimental details were shown as follows: 0.1 g of the sample was dispersed into 10 mL of MO solution (20 mg/L) in a disk with a diameter of ca. 5 cm. The solution was allowed to reach an adsorption–desorption equilibrium among the photocatalyst, MO, and water before visible-light irradiation. A 350 W xenon lamp equipped with a UV-cutoff filter (providing visible light with $\lambda \geq 400$ nm) was used as a visible-light source. The average light intensity striking the surface of the reaction solution was about 40 mW cm^2. The concentration of MO was determined by an UV–visible spectrophotometer (UV-1240, SHI-MADZU, Japan). After visible-light irradiation for some time, the reaction solution was centrifuged to measure the concentration of MO. As for the methyl orange aqueous solution with low concentration, its photocatalytic decolorization is a pseudo-first-order reaction and its kinetics may be expressed as $\ln(c_0/c) = kt$, where k is the apparent rate constant, and c_0 and c are the methyl orange concentrations at initial state and after irradiation for t min, respectively [21,27].

3. Results and discussion

3.1. Morphology and microstructures

Fig. 1A and B shows the FESEM images of the AgBr particles before and after surface modification by Fe(III) cocatalyst. It is clear that the direct participation reaction method results in a wide particle-size distribution (0.3–1.5 μm) of the AgBr particles (Fig. 1A). The corresponding XRD pattern (Fig. 1C) suggests the formation of AgBr phase (JCPDS no. 06-0438). As for the Fe(III)/AgBr photocatalyst, it is clear that there is no obvious change for the morphology of the resultant Fe(III)/AgBr (Fig. 1B) owing to a low-temperature modification process (60 °C). Moreover, in view of a low-concentration $Fe(NO_3)_3$ solution, no related diffraction peaks of Fe(III) compounds can be detected (Fig. 1C).

As the surface modification process of AgBr by Fe(III) cocatalyst is performed at a low temperature (60 °C), it is believed that these

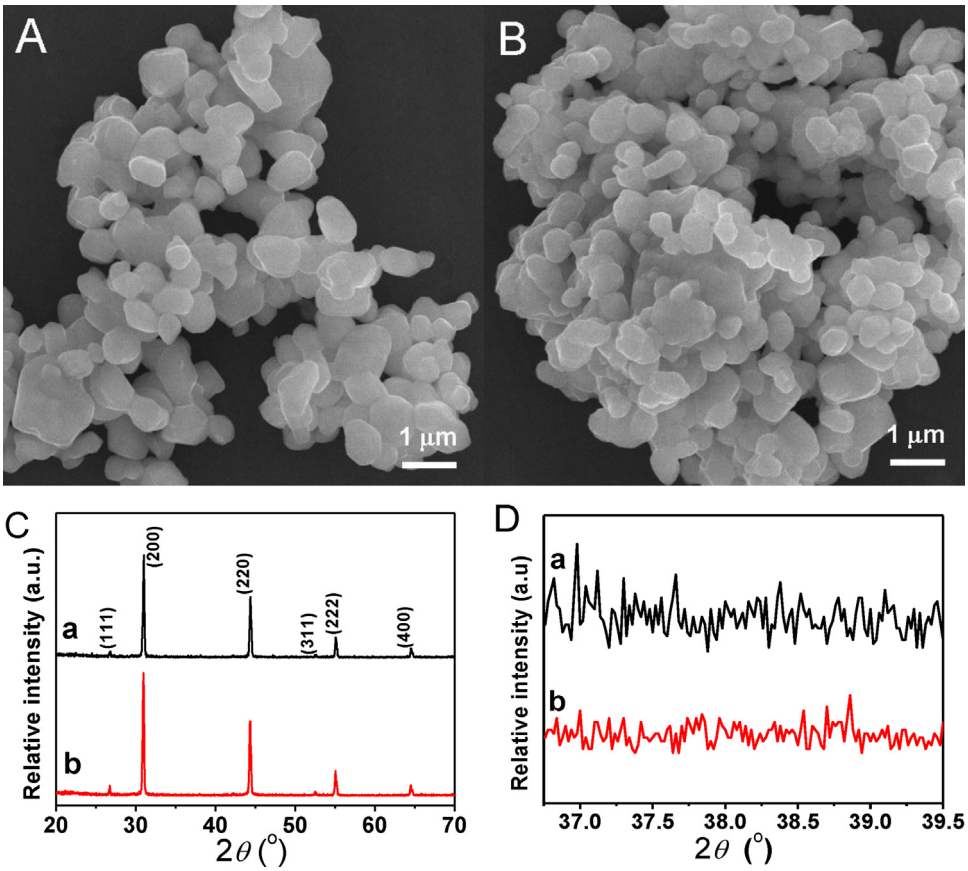

Fig. 1. SEM images of (A) AgBr and (B) Fe(III)/AgBr (0.05 M) samples; (C) XRD patterns and (D) their corresponding diffraction peaks of metallic Ag for the (a) AgBr and (b) Fe(III)/AgBr (0.05 M) samples.

Fe(III) ions may exist only on the surface of AgBr and cannot be doped into the lattices of AgBr. XPS, a surface sensitive technique, was used to analyze the elemental composition of AgBr particles before and after loading of Fe(III) cocatalyst. Fig. 2A shows the XPS survey spectra of the AgBr and Fe(III)/AgBr. Compared with the pure AgBr sample (Fig. 2A-a), new XPS peaks of Fe element are found in the Fe(III)/AgBr sample (Fig. 2A-b) in addition to the Ag, Br, C and O elements. The Ag and Br XPS peaks are from the AgBr powder, while the C element can be contributed to the adventitious hydrocarbon from XPS instrument itself. To further investigate the chemical state of Fe element, the high-resolution XPS spectrum of the Fe 2p of the Fe(III)/AgBr was shown in Fig. 2B. It is clear that the binding energies of Fe $2p_{3/2}$ and Fe $2p_{1/2}$ are located at ca. 711.4 and 724.9 eV, respectively, which can be ascribed to Fe(III) ions [31,32]. Fig. 2C shows the Ag 3d XPS spectrum of the AgBr and Fe(III)/AgBr. The binding energies of Ag $3d_{5/2}$ and Ag $3d_{3/2}$ are located at 367.8 and 373.8 eV, respectively, which can be mainly attributed to the Ag^+ ions [27,33]. The same binding energy of the AgBr and Fe(III)/AgBr photocatalysts suggests that the Fe(III)-cocatalyst modification cannot obviously effect the surface microstructures of AgBr phase.

It is very important and interesting to determine the microstructures of Fe(III) cocatalyst loaded on the surface of AgBr particles. However, owing to a very limited amount of Fe element grafted on the surface of AgBr particles, it is difficult to determine the real chemical state of Fe(III) cocatalyst. In our previous study, the loaded Fe species were demonstrated to be in the 3+ state and showed an amorphous FeO(OH)-like structure in the Fe(III)/TiO_2 photocatalyst [30]. In this study, it is found that the intensity of O 1s XPS peak have an obvious increase after loading Fe(III) cocatalyst, as shown in Fig. 2A. According to the element compositions based on the XPS results, the amount of Fe and O element was 7.9 and 24.8 at.%, respectively. Therefore, the ratio of Fe to O element can be calculated to be 3.1. Considering a small amount of O element in the pure AgBr sample which is possibly from the adsorbed water during preparation, it can be deduced that the real ratio of Fe to O element should be lower than 3.1. In addition, in view of a lower synthetic temperature (60 °C) in this study than that of our reported Fe(III)/TiO_2 photocatalyst (90 °C), it is believed that the present Fe(III) cocatalyst can be existed in an amorphous $Fe(OH)_3$ cluster structure [30]. Based on the XPS results, when the $Fe(NO_3)_3$ concentration was controlled to be 0, 0.001, 0.005, 0.01, and 0.05 mol L^{-1}, the Fe amount on the Fe(III)/AgBr surface can be calculated to be 0, 1.3, 7.9, 12.5 and 15.6 at.%, respectively.

The successful loading of Fe(III) cocatalyst on the AgBr photocatalyst can be further demonstrated by UV–vis spectra, as shown in Fig. 3. It is clear that in addition to its band-gap absorption at ca. 350–470 nm, the AgBr sample also shows obvious surface plasmon resonance absorption of Ag nanoparticles at 450–800 nm [7,21], suggesting that the AgBr is very instable and can be easily decomposed into metallic Ag. After surface modification of AgBr by Fe(III) cocatalyst, the resultant Fe(III)/AgBr samples show no surface plasmon resonance absorption of metallic Ag nanoparticles, suggesting the effective inhibition of AgBr photodecomposition by Fe(III) cocatalyst. With increasing amount of Fe(III) cocatalyst, there is a gradually increased absorption in the visible-light region of 470–650 nm, which can be mainly attributed to the d-d transition of Fe(III) ions in the amorphous $Fe(OH)_3$ clusters [34]. In addition, the interfacial charge transfer (IFCT) absorption from the VB of AgBr to Fe(III) cocatalyst also possibly contributes to the enhanced visible-light absorption [30].

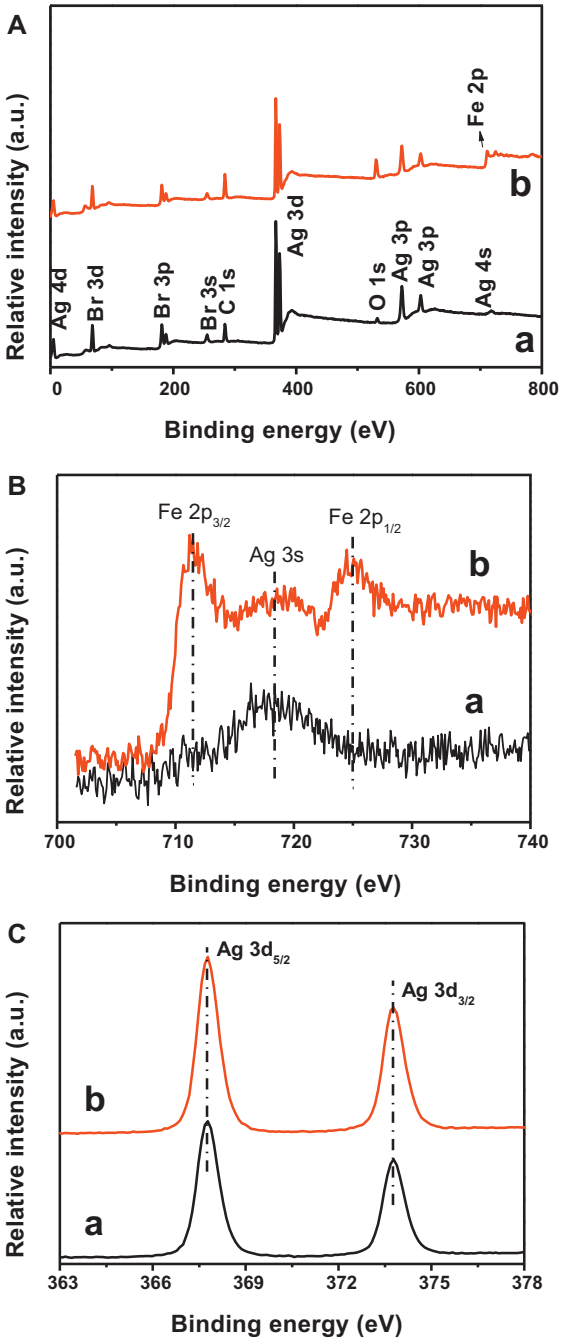

Fig. 2. (A) XPS survey spectra and the high-resolution XPS spectra of (B) Fe 2p and (C) Ag 3d: (a) AgBr; (b) Fe(III)/AgBr (0.05 M).

3.2. Enhanced photocatalytic activity of AgBr by Fe(III) cocatalyst

The photocatalytic performance of AgBr and Fe(III)/AgBr samples were evaluated by photocatalytic decolorization of MO aqueous solution under visible-light irradiation, as shown in Fig. 4. In the dark, no change in the concentration of MO was observed in the presence of AgBr and Fe(III)/AgBr photocatalysts. Furthermore, visible-light illumination in the absence of photocatalysts did not result in the photocatalytic decolorization of MO. It is clear that the AgBr shows a high photocatalytic activity for the decomposition of MO solution and the corresponding rate constant (k) can be calculated to be 0.056 min^{-1}. After the AgBr particles are modified by Fe(III) cocatalyst, the resulting Fe(III)/AgBr photocatalysts exhibit a remarkably enhanced photocatalytic performance. Especially,

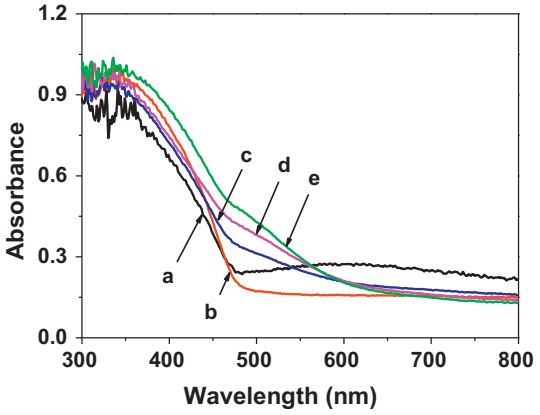

Fig. 3. UV–vis spectra of (a) AgBr; (b) Fe(III)/AgBr (0.01 M); (c) Fe(III)/AgBr (0.05 M); (d) Fe(III)/AgBr (0.1 M); (e) Fe(III)/AgBr (0.5 M).

when the $Fe(NO_3)_3$ concentration increased to 0.005 mol L^{-1}, the prepared Fe(III)/AgBr (0.05 M) photocatalyst shows an enhanced photocatalytic activity with a rate constant of 0.132 min^{-1}, which is obviously higher than the AgBr particles by a factor of 2.35. However, further increase of the $Fe(NO_3)_3$ concentration results in an obviously decreased performance of the Fe(III)/AgBr photocatalysts. This phenomenon is in good agreement with the reported cocatalyst-modified photocatalysts such as Fe(III)/TiO_2 and Cu(II)/TiO_2 [30]. As the reduction reactions of photogenerated electrons and the oxidation reactions of photogenerated holes occur on the different surface active sites, an optimal amount of cocatalyst can contribute to a rapid separation of photogenerated charges, resulting in an enhanced photocatalytic performance. However, further increasing Fe(III) cocatalyst amount on the photocatalyst surface can decrease the number of oxidation active sites of photogenerated holes, leading to a decreasing photocatalytic activity.

To investigate the performance stability of the Fe(III)/AgBr photocatalyst, recycle experiments of MO decomposition were performed and the corresponding results are shown in Fig. 5A. It is clear that the Fe(III)/AgBr (0.05 M) photocatalyst shows a gradually decreased photocatalytic performance during repeated photocatalytic reactions. However, after three cycles of the photocatalytic tests, it is interesting to find that the Fe(III)/AgBr photocatalyst shows a comparable rate constant for the following repeated experiment, suggesting the formation of a stable photocatalytic performance of the Fe(III)/AgBr photocatalyst. Similar deactivation process can also be found in the um-modified AgBr photocatalyst (Fig. 5B), which is in good agreement with our previous

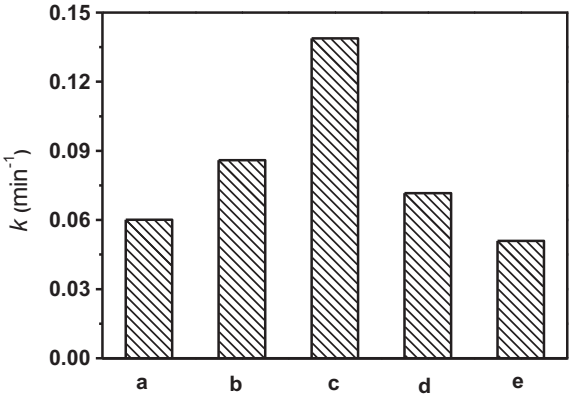

Fig. 4. The rate constant (k) of MO solution by various photocatalysts: (a) AgBr, (b) Fe(III)/AgBr (0.01 M), (c) Fe(III)/AgBr (0.05 M), (d) Fe(III)/AgBr (0.1 M), and (e) Fe(III)/AgBr (0.5 M).

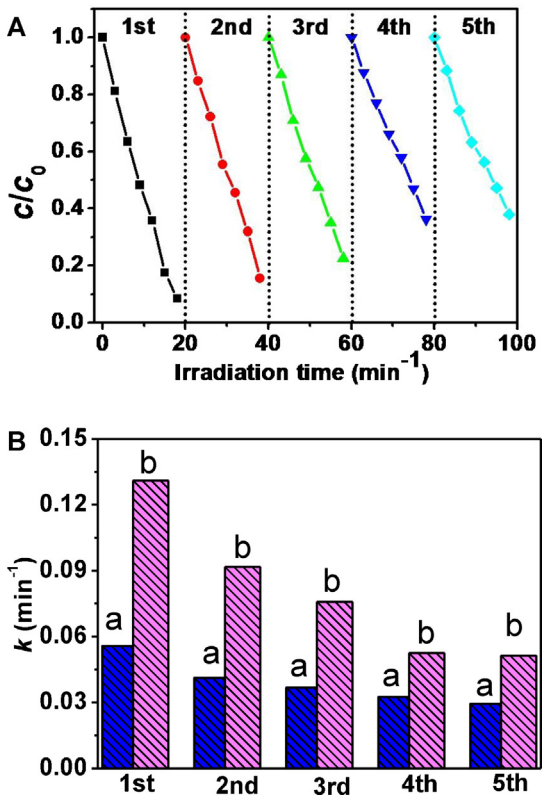

Fig. 5. (A) The repeated photocatalytic decomposition of MO for the Fe(III)/AgBr (0.05 M) photocatalyst; (B) the compared photocatalytic performance of the (a) AgBr and (b) Fe(III)/AgBr (0.05 M) photocatalysts.

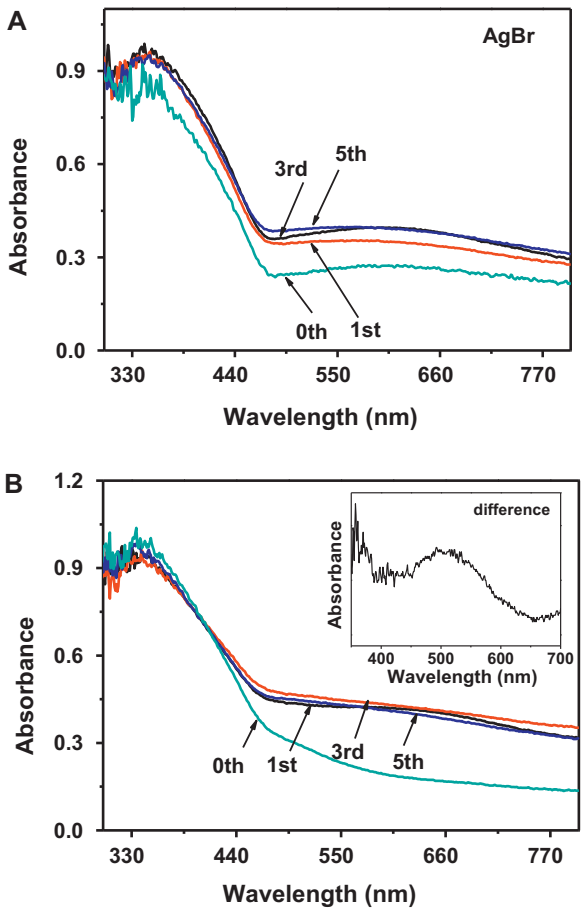

Fig. 6. UV–vis spectra of (A) AgBr and (B) Fe(III)/AgBr (0.05 M) photocatalysts after different-cycle photocatalytic test. The inset in (B) shows the difference UV–vis spectrum between third-cycle and as-prepared Fe(III)/AgBr (0.05 M) sample.

results about the Ag-based photocatalysts such as AgI and Ag_2O [17,24]. However, it should be noted that all the photocatalytic activities of the Fe(III)/AgBr photocatalyst is higher than that of the corresponding AgBr sample during repeating tests (Fig. 5B). To compare and evaluate the finally stable photocatalytic performance, in this study, the fifth repeated activities of the AgBr and Fe(III)/AgBr photocatalysts are compared and their corresponding rate constants can be calculated to be 0.030 and 0.052 min^{-1}, respectively (Fig. 5B). Clearly, the Fe(III)/AgBr photocatalyst obviously shows a higher photocatalytic activity than the AgBr particles by a factor of 1.73. Therefore, the Fe(III) can act as an efficient cocatalyst for the improved photocatalytic performance of AgBr photocatalyst.

3.3. Enhanced photoinduced stability of AgBr by Fe(III) cocatalyst

It is well known that a photocatalyst for practical applications should have good photoinduced stability under visible-light irradiation in addition to its perfect photocatalytic performance. However, extensive investigations have demonstrated that pure AgBr is a photosensitive material and can be partially decomposed into metallic Ag during visible-light irradiation owing to its photoinduced instability [11,12,35]. To investigate the effect of Fe(III) cocatalyst on the photoinduced stability of AgBr photocatalysts, after repeated photocatalytic reactions, the resultant AgBr and Fe(III)/AgBr samples were first analyzed by UV–vis spectra. Fig. 6A shows the UV–vis spectra of the AgBr photocatalysts after different-cycle photocatalytic test. It is found that, with increasing repetitions to three times, there is a gradual enhancement of the plasmon absorption at 450–800 nm, suggesting the gradually increasing amount of metallic Ag phase. However, when the photocatalytic test further increases from three to five times, the intensity of the plasmon absorption has no obvious change. Considering the great influence of the plasmon absorption of Ag nanoparticles by their shape, size, amount and dielectric environment [36,37], the negligible change of the UV–vis spectra suggests that there is no obvious difference about the size and number of the Ag phase after a third-cycle photocatalytic reaction. A similar change of UV–vis spectra can also be observed in the Fe(III)/AgBr photocatalyst (Fig. 6B). However, compared with the AgBr photocatalyst, the intensity of the plasmon resonance absorption of metallic Ag nanoparticles at 450–800 nm has a remarkable decrease in the Fe(III)/AgBr photocatalyst, suggesting that less metallic Ag is produced during repeated photocatalytic reaction. Therefore, it is clear that the photoinduced stability of photosensitive AgBr particles can be greatly improved by the surface loading of Fe(III) cocatalyst. However, it should be noted that the difference UV–vis spectrum of the Fe(III)/AgBr photocatalyst before and after a third-cycle decomposition reaction (inset in Fig. 6B) clearly suggests the formation of a small amount of metallic Ag owing to its plasmon resonance absorption.

The enhanced photoinduced stability of AgBr phase by Fe(III) cocatalyst can be further demonstrated by XRD and XPS technologies. With increasing repetitions of the photocatalytic reaction, both of the resultant AgBr and Fe(III)/AgBr samples (not shown here) show similar wide-angle diffraction peaks as the as-prepared AgBr and Fe(III)/AgBr photocatalysts (Fig. 1C), suggesting that the AgBr and Fe(III)/AgBr samples cannot be destroyed completely under visible-light irradiation, in good agreement with the reported silver halides [12]. Based on the results of UV–vis spectra (Fig. 6), after three successive photocatalytic reactions, the resultant AgBr

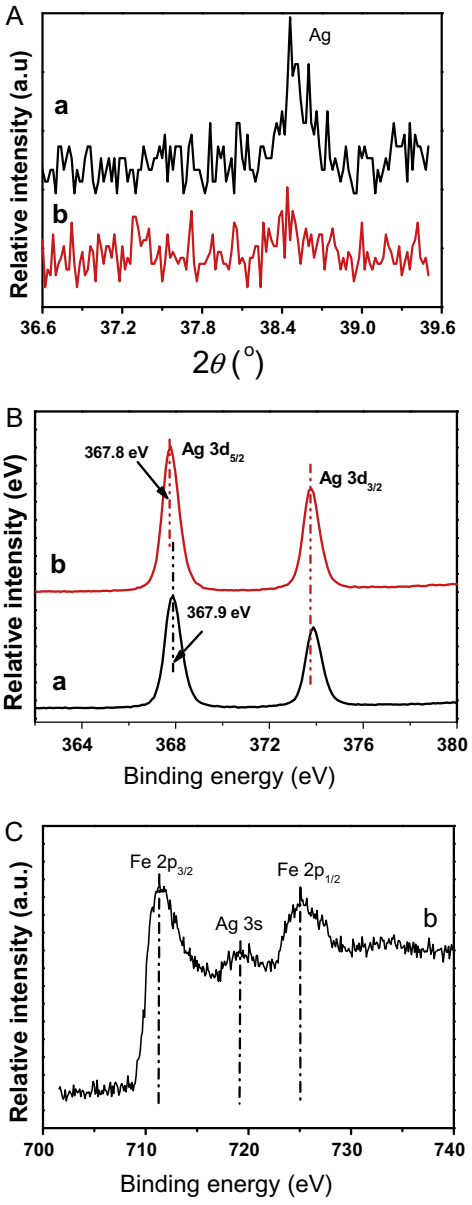

Fig. 7. (A) XRD patterns of the diffraction peak of metallic Ag; XPS spectra of (B) Ag 3d and (C) Fe 2p: (a) AgBr and (b) Fe(III)/AgBr (0.05 M) photocatalysts after three-cycle photocatalytic tests.

and Fe(III)/AgBr photocatalysts can be regarded as typical and stable structures, which are further investigated by XRD (Fig. 7A) and XPS (Fig. 7B). It is clear that, compared with the obvious diffraction peak of metallic Ag in the bare AgBr particles, the Fe(III)/AgBr photocatalyst shows a significantly decreased intensity, suggesting the formation of less amount of metallic Ag phase (Fig. 7A). Fig. 7B shows the XPS Ag spectra of the AgBr and Fe(III)/AgBr photocatalysts obtained after three-cycle photocatalytic test. It is found that the AgBr photocatalyst shows a slightly higher binding energy (367.9) than the Fe(III)/AgBr sample (367.8 eV) owing to the formation of more metallic Ag phase with a larger binding energy [21,38]. The amount of metallic Ag in the AgBr and Fe(III)/AgBr photocatalysts after three-cycle photocatalytic test can be calculated to be 8.2 and 2.9 at.%, respectively, based on the XPS results. Therefore, it is clear that the photoinduced stability of AgBr phase can be greatly improved by the surface loading of Fe(III) cocatalyst. In addition, compared with the as-prepared Fe(III)/AgBr photocatalyst (Fig. 2B), it is found that there is no change for the XPS Fe(III) spectrum of

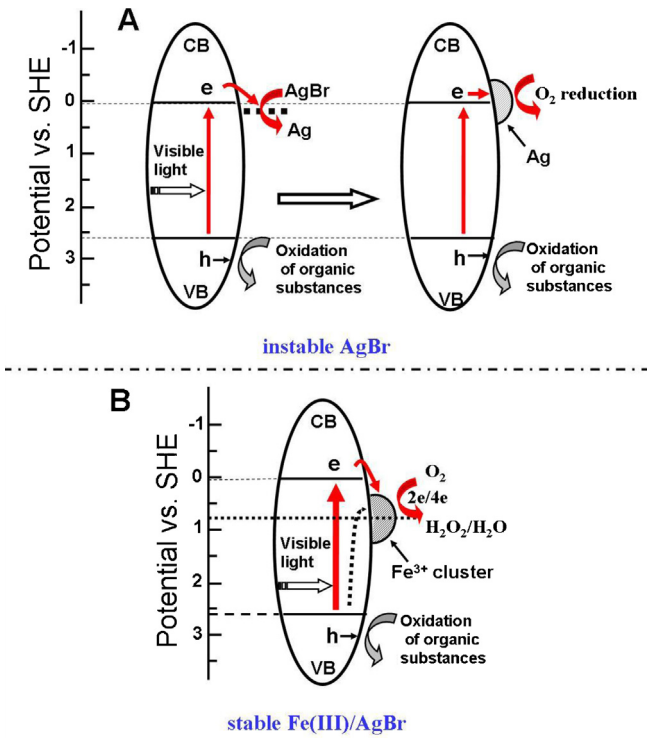

Fig. 8. Schematic diagrams showing the possible photocatalytic mechanism of (A) AgBr and (B) Fe(III)/AgBr photocatalysts: (A) the photogenerated electrons are captured by Ag^+ ions in AgBr lattices, resulting in the rapid decomposition of AgBr and the formation of metallic Ag; (B) the photogenerated electrons are easily transferred to the oxygen via Fe(III) cocatalyst grafted on the AgBr surface, effectively preventing the rapid formation of metallic Ag.

Fe(III)/AgBr photocatalysts after three-cycle photocatalytic reactions (Fig. 7C), indicating the stable structure of the Fe(III) cocatalyst during photocatalytic reactions. In addition, the amount of Fe element can be calculated to be 7.6 at.%, similar to the as-prepared Fe(III)/AgBr photocatalyst.

3.4. Photocatalytic mechanism

The above results highlight an interesting phenomenon of enhanced photoinduced stability and photocatalytic activity of AgBr photocatalyst by surface modification of Fe(III) cocatalyst. To investigate the potential mechanism of Fe(III)/AgBr photocatalyst, the CB energy level of AgBr can be calculated according to the equation of $E_c = -\chi + 0.5E_g$, where E_c, χ and E_g are the CB energy level, absolute electronegativity and band gap of semiconductor, respectively [39]. Therefore, the CB and VB energy levels of AgBr are calculated to be ca. 0.05 V and 2.55 V (vs SHE), respectively. Fig. 8A shows the possible photocatalytic mechanism of bare AgBr photocatalyst and its corresponding self-stabilizing process during repeated photocatalyst reaction. When the bare AgBr photocatalyst is irradiated with visible-light light, the photogenerated electrons are produced on the CB of AgBr particles while photogenerated holes remain in its VB. In view of a more positive potential of AgBr/Ag (0.0711 V, vs. SHE) [40] than the CB potential (0.05 V, vs. SHE) of AgBr, the photogenerated electrons are preferably transferred to the surface lattice Ag^+ in AgBr. Therefore, the surface Ag^+ ions in AgBr lattice can be in situ reduced by photogenerated electrons to form metallic Ag under visible-light irradiation (Fig. 8A), as suggested by the XRD, UV–vis and XPS results (Figs. 6 and 7). However, once a certain amount of metallic Ag is formed on the surface of AgBr nanoparticles, the following photocatalytic mechanism is changed; namely, the photogenerated electrons tend to transfer to

the metallic Ag sites and then are captured by oxygen (Fig. 8A). Owing to a more effective capture of photogenerated electrons by the lattice Ag^+ ions in the AgBr (AgBr/Ag = 0.0711 V, vs. SHE) than the oxygen (O_2/HO_2 = −0.0711 V, vs. SHE) [40] via metallic Ag, the bare AgBr photocatalyst shows the highest decomposition rate of organic substances for the first-time cycle. With increasing cyclic tests, the initial decrease of photocatalytic activity of the bare AgBr photocatalyst can be attributed to the rapid formation of metallic Ag, while after three-time photocatalytic test, the subsequently stable activity corresponds to the formation of a stable Ag–AgBr composite photocatalyst (Figs. 6B and 8A). As for the Fe(III)/AgBr photocatalyst, a similar deactivation process during repeated photocatalytic reactions can also be found, and the main reason can be attributed to the formation of a small amount of metallic Ag. Therefore, it is clear that the photoinduced stability of bare AgBr structure can be enhanced by in situ decomposited Ag arising from the photosensitive AgBr. The self-stability phenomenon is in good agreement with our reported Ag_2O and AgI photocatalysts [17,24].

After surface modification of bare AgBr by Fe(III) cocatalyst, the photocatalytic performance and photoinduced stability of the AgBr can be greatly improved. Considering a more positive potential of Fe^{3+}/Fe^{2+} (0.771 V, vs. SHE) than the AgBr/Ag (0.0711 V, vs. SHE) [40], it is obvious that the photogenerated electrons in the CB of AgBr can easily transfer to the Fe(III) cocatalyst. Owing to the rapid transfer of photogenerated electrons from AgBr phase to Fe(III) cocatalyst, the resultant holes in the VB can oxidize organic compounds with a higher efficiency. On the other hand, after accepting a photogenerated electron, the Fe(III) ion transfers into Fe(II). It is well known that the Fe(II) ions are unstable and easily become Fe(III) through the reduction of oxygen under ambient conditions ($4Fe^{2+} + O_2 + 4H^+ \rightarrow 4Fe^{3+} + 2H_2O$ or $4Fe^{2+} + O_2 + 2H_2O \rightarrow 4Fe^{3+} + 4OH^-$) [40], namely, the Fe(III) can be well recovered via the effective oxidation of Fe(II) by oxygen. In view of a more positive potential (0.771 V, vs SHE) [40] of Fe^{3+}/Fe^{2+} than the single-electron reduction of oxygen ($O_2 + e^- + H^+ = HO_2$ (aq), −0.046 V vs. SHE) [40], the Fe(III) cocatalyst possibly reduces oxygen via multi-electron transfer routes ($O_2 + 2e^- + 2H^+ = H_2O_2$ (aq), +0.682 V vs. SHE; $O_2 + 4e^- + 4H^+ = 2H_2O$ (aq), +1.23 V vs. SHE) [40]. A similar multi-electron oxygen reduction was also found on the Cu(II) [41,42], Ag_2O [33] and Pt [43] cocatalysts. As a consequence, the photogenerated electrons in the CB of AgBr can be rapidly transferred to the Fe(III) cocatalyst, while the producing Fe(II) ions effectively reduce adsorbed oxygen, leading the enhanced photocatalytic performance and photoinduced stability of AgBr.

In our previous study about the Fe(III)/TiO_2 photocatalyst, it was found that the electrons on the VB of TiO_2 could be transferred into Fe(III) clusters via the IFCT mechanism under visible-light irradiation, causing the effective decomposition of organic substances [30]. In this study, the IFCT absorption of the Fe(III)/AgBr photocatalysts also possibly contribute the enhanced photocatalytic activity (Fig. 8B). However, compared with the strong band-gap absorption of AgBr, the IFCT absorption of the Fe(III)/AgBr photocatalyst should be very limited because the IFCT can only function between the interface of AgBr and Fe(III) cocatalyst.

4. Conclusions

Fe(III) cocatalyst was successfully grafted on the surface of AgBr particles by an impregnation method and was demonstrated to be a new and efficient cocatalyst to significantly improve the photocatalytic activity and photoinduced stability of AgBr photocatalyst. Owing to a more effective transfer of photogenerated electrons from the CB of AgBr to Fe(III) cocatalyst than the lattice Ag^+ in AgBr, the decomposition reaction of AgBr and the formation of metallic Ag can be greatly prohibited, resulting in the enhanced photocatalytic activity and photoinduced stability. Compared with the well-known noble metal cocatalysts (e.g., Pt, Au, Ag), the present abundant and cheap Fe(III) cocatalyst can be regarded as one of the ideal cocatalysts for the smart design and development of high-performance photocatalytic materials. In addition, considering the effective inhibition effect for the rapid decomposition of photosensitive materials by surface cocatalyst, the work may provide a new insight for the potential applications of various photosensitive Ag-based materials.

Acknowledgments

This work was partially supported by the National Natural Science Foundation of China (21277107, 61274129, and 51208396). This work was also financially supported by the 973 Program (2013CB632402), 863 Program (2012AA062701), the Natural Science Foundation of Hubei Province (2012FFB05002), the Project-sponsored by SRF for ROCS, SEM and Fundamental Research Funds for the Central Universities (Grants 2013-1a-039 and 2013-1a-036).

References

[1] C.C. Chen, W.H. Ma, J.C. Zhao, Chemical Society Reviews 39 (2010) 4206–4219.
[2] Q.J. Xiang, J.G. Yu, M. Jaroniec, Chemical Society Reviews 41 (2012) 782–796.
[3] M.R. Hoffmann, S.T. Martin, W. Choi, D.W. Bahnemann, Chemical Reviews 95 (1995) 69–96.
[4] S.G. Kumar, L.G. Devi, Journal of Physical Chemistry A 115 (2011) 13211–13241.
[5] A. Fujishima, X.T. Zhang, D.A. Tryk, Surface Science Reports 63 (2008) 515–582.
[6] A.L. Linsebigler, G. Lu, J.T. Yates, Chemical Reviews 95 (1995) 735–758.
[7] P. Wang, B.B. Huang, X.Y. Qin, X.Y. Zhang, Y. Dai, J.Y. Wei, M.H. Whangbo, Angewandte Chemie-International Edition 47 (2008) 7931–7933.
[8] P. Wang, B.B. Huang, Z.Z. Lou, X.Y. Zhang, X.Y. Qin, Y. Dai, Z.K. Zheng, X.N. Wang, Chemistry: A European Journal 16 (2010) 538–544.
[9] Y.P. Bi, J.H. Ye, Chemical Communications 46 (2010) 1532–1534.
[10] P. Wang, B.B. Huang, X.Y. Zhang, X.Y. Qin, H. Jin, Y. Dai, Z.Y. Wang, J.Y. Wei, J. Zhan, S.Y. Wang, J.P. Wang, M.H. Whangbo, Chemistry: A European Journal 15 (2009) 1821–1824.
[11] Y.Q. Lan, C. Hu, X.X. Hu, J.H. Qu, Applied Catalysis B: Environmental 73 (2007) 354–360.
[12] N. Kakuta, N. Goto, H. Ohkita, T. Mizushima, Journal of Physical Chemistry B 103 (1999) 5917–5919.
[13] X.X. Hu, C. Hu, T.W. Peng, X.F. Zhou, J.H. Qu, Environmental Science & Technology 44 (2010) 7058–7062.
[14] X.F. Zhou, C. Hu, X.X. Hu, T.W. Peng, J.H. Qu, Journal of Physical Chemistry C 114 (2010) 2746–2750.
[15] Y.P. Bi, H.Y. Hu, S.X. Ouyang, G.X. Lu, J.Y. Cao, J.H. Ye, Chemical Communications 48 (2012) 3748–3750.
[16] Z.G. Yi, J.H. Ye, N. Kikugawa, T. Kako, S.X. Ouyang, H. Stuart-Williams, H. Yang, J.Y. Cao, W.J. Luo, Z.S. Li, Y. Liu, R.L. Withers, Nature Materials 9 (2010) 559–564.
[17] X.F. Wang, S.F. Li, H.G. Yu, J.G. Yu, S.W. Liu, Chemistry: A European Journal 17 (2011) 7777–7780.
[18] G.P. Dai, J.G. Yu, G. Liu, Journal of Physical Chemistry C 116 (2012) 15519–15524.
[19] W.G. Wang, B. Cheng, J.G. Yu, G. Liu, W.H. Fan, Chemistry: An Asian Journal 7 (2012) 1902–1908.
[20] Y.P. Liu, L. Fang, H.D. Lu, Y.W. Li, C.Z. Hu, H.G. Yu, Applied Catalysis B: Environmental 115 (2012) 245–252.
[21] X.F. Wang, S.F. Li, Y.Q. Ma, H.G. Yu, J.G. Yu, Journal of Physical Chemistry C 115 (2011) 14648–14655.
[22] X.F. Wang, S.F. Li, H.G. Yu, J.G. Yu, Journal of Molecular Catalysis A: Chemical 334 (2011) 52–59.
[23] J.G. Yu, G.P. Dai, B.B. Huang, Journal of Physical Chemistry C 113 (2009) 16394–16401.
[24] H.G. Yu, L. Liu, X.F. Wang, P. Wang, J.G. Yu, Y.H. Wang, Dalton Transactions 41 (2012) 10405–10411.
[25] J.W. Mitchell, Reports on Progress in Physics 20 (1957) 433–515.
[26] J.G. Yu, J.F. Xiong, B. Cheng, S.W. Liu, Applied Catalysis B: Environmental 60 (2005) 211–221.
[27] R. Liu, P. Wang, X.F. Wang, H.G. Yu, J.G. Yu, Journal of Physical Chemistry C 116 (2012) 17721–17728.
[28] Z.G. Zhao, M. Miyauchi, Angewandte Chemie-International Edition 47 (2008) 7051–7055.
[29] P. Wang, J. Wang, X.F. Wang, H.G. Yu, J.G. Yu, M. Lei, Y.G. Wang, Applied Catalysis B: Environmental 132–133 (2013) 452–459.
[30] H.G. Yu, H. Irie, Y. Shimodaira, Y. Hosogi, Y. Kuroda, M. Miyauchi, K. Hashimoto, Journal of Physical Chemistry C 114 (2010) 16481–16487.

[31] B. Rajesh, N. Sasirekha, Y.-W. Chen, Journal of Molecular Catalysis A: Chemical 275 (2007) 174–182.
[32] R. Supplit, N. Husing, H. Bertagnolli, M. Bauer, V. Kessler, G.A. Seisenbaeva, S. Bernstorff, S. Gross, Journal of Materials Chemistry 16 (2006) 4443–4453.
[33] H.G. Yu, R. Liu, X.F. Wang, P. Wang, J.G. Yu, Applied Catalysis B: Environmental 111 (2012) 326–333.
[34] O.G. Holmes, D.S. Mcclure, Journal of Chemical Physics 26 (1957) 1686–1694.
[35] C. Hu, Y.Q. Lan, J.H. Qu, X.X. Hu, A.M. Wang, Journal of Physical Chemistry B 110 (2006) 4066–4072.
[36] E.M. Larsson, J. Alegret, M. Kall, D.S. Sutherland, Nano Letters 7 (2007) 1256–1263.
[37] A.D. McFarland, R.P. Van Duyne, Nano Letters 3 (2003) 1057–1062.
[38] Y.Z. Li, H. Zhang, Z.M. Guo, J.J. Han, X.J. Zhao, Q.N. Zhao, S.J. Kim, Langmuir 24 (2008) 8351–8357.
[39] Y. Xu, M.A.A. Schoonen, American Mineralogist 85 (2000) 543–556.
[40] A.J. Bard, R. Parsons, J. Jordan, Standard Potentials in Aqueous Solution, Marcel Dekker, New York, 1985.
[41] H.G. Yu, H. Irie, K. Hashimoto, Journal of the American Chemical Society 132 (2010) 6898–6899.
[42] H. Irie, S. Miura, K. Kamiya, K. Hashimoto, Chemical Physics Letters 457 (2008) 202–205.
[43] R. Abe, H. Takami, N. Murakami, B. Ohtani, Journal of the American Chemical Society 130 (2008) 7780–7781.